



Full Length Article

Evaluation of Antifungal Mechanism of *Bacillus amyloliquefaciens* BA-16-8

Ruimin Fu¹, Hong Zhang², Huiping Chang¹, Fuming Zhang³ and Wuling Chen⁴

¹Department of Life Science, Henan Finance University, Zhengzhou, Henan, China

²Department of Science, Henan Finance University, Zhengzhou, Henan, China

³Center for Biotechnology and Interdisciplinary Studies, Rensselaer Polytechnic Institute, Troy, New York, USA

⁴Microbiology Engineering Institute, Shaanxi Normal University, Xi'an, shaanxi, China

*For correspondence: angelaminmin@163.com

Received 19 August 2019; Accepted 1 October 2019; Published 16 January 2020

Abstract

Penicillium expansum, the pathogen in apple blue mold, is the primary cause of postharvest apple decay. Fengycin produced by *Bacillus amyloliquefaciens* BA-16-8 can inhibit the growth of *P. expansum*. In this study, we explored the antifungal mechanism of fengycin against *P. expansum*. The effects of fengycin on the morphological structure of *P. expansum* mycelium were studied via scanning electron microscopy and transmission electron microscopy. The effect of fengycin on the DNA of *P. expansum* was investigated by conducting electrophoretic mobility shift assay (EMSA). Results showed that after fengycin treatment, the surface of *P. expansum* became rough and the intracellular protoplasm, particularly the mitochondrion, was damaged by fengycin. EMSA results showed that fengycin can bind nonspecifically with the DNA of *P. expansum* *in vitro*. Hence, fengycin can inhibit *P. expansum* mycelium by altering its cell membrane integrity and binding with its DNA. © 2020 Friends Science Publishers

Keyword: Antifungal mechanism; *Bacillus amyloliquefaciens*; Fengycin; *Penicillium expansum*

Introduction

Penicillium expansum is the primary pathogen that causes postharvest apple decay. *P. expansum* can be extracted from nearly all rotten apples (Rozas *et al.* 2019). When apples are attributed to mutual collisions during storage or transportation, *P. expansum* spores hidden on the fruit surface may intrude into fruits through injuries and produce mycelium, which may cause fruit rotting. Furthermore, the secondary metabolites of *P. expansum* may pose threats to human health and cause serious food safety problems (Moosa *et al.* 2019). At present, the activities and toxin accumulation of pathogenic fungus are primarily controlled by spraying chemical bactericides (Crossley 1976). However, most chemical fungicides have demonstrated potential carcinogenicity. The long-term use of these chemicals may cause environmental pollution and drug resistance of pathogenic fungus. Therefore, screening highly efficient, nontoxic, and safe antagonistic microbe with broad-spectrum activities and using them to guarantee the freshness of apple in storage have been considered a safe and efficient technology in field of fruit and vegetable storage (Mohammadi and Salouti 2015).

Our laboratory separated one strain of *Bacillus amyloliquefaciens* BA-16 that can effectively resist *P. expansum* from apple surface. The mutant strain, BA-16-8,

which exhibits significantly enhanced antagonistic activity, was acquired through mutation breeding (Fu *et al.* 2016a). The results of high-performance liquid chromatography (HPLC) and mass spectrometry showed that the mycoproteins produced by BA-16-8 are mostly the lipopeptide antibiotics fengycin and surfactin. Fengycin is a key substance that inhibits *P. expansum* (Fu *et al.* 2016b).

Fengycin is an inner ester ring structure formed by the cross-linking of cyclic peptides; it comprises 10 amino acids and α -fatty acid chains. Fengycin can strongly inhibit filamentous fungi. However, no consensus has yet been reached concerning its specific inhibition mechanism (Costa *et al.* 2018). The structure of fengycin exhibits many similarities to those of polyene antifungal antibiotics, such as natamycin. All these antibiotics are classified as macrolides. Ferraz *et al.* (2019) pointed out that natamycin is conducive to identifying the antimicrobial mechanism of fengycin. Natamycin interacts with ergosterol on the cytomembrane of pathogenic fungus through conjugated double bonds in macrolides, and thus, the permeability of the membrane is changed. Using natamycin as reference, Wachenforff *et al.* proposed that fengycin destroys membrane permeability through sterols that act on filamentous fungal cell membrane (Srikhong *et al.* 2018; Villegas-Escobar *et al.* 2018). However, several problems should be discussed further, such as whether fengycin can

influence other structures of the membrane apart from sterols, whether fengycin exerts other destructive effects on pathogenic fungi aside from changing membrane permeability, and whether fengycin exhibits specificity to the binding sites of filamentous fungal membrane.

In the current study, variations in the external morphologies and damage degree of *P. expansum* cell structure caused by fengycin were explored via scanning electron microscopy (SEM) and transmission electron microscopy (TEM). The effects of fengycin on the genome DNA of *P. expansum* were analyzed via gel retardation. The research results can provide corresponding theoretical references and technological support for the development and application of fengycin to the postharvest biological storage of apple.

Materials and Methods

Bacterial strains and reagents

The bacterial strain for fengycin production, i.e., *B. amyloliquefaciens* BA-16-8, was isolated and bred in the Biological Engineering Laboratory of Northwest University, China.

The indicator fungus, namely, *P. expansum*, was provided by the Shanxi Institute of Microbiology, Chinese Academy of Sciences.

Potato dextrose broth (PDB) and potato dextrose agar (PDA) were prepared following the methods presented in Beld *et al.* (2014) and Tanaka *et al.* (2014). Natamycin was provided by Sigma-Aldrich Corporation. KYKY-EM600 scanning electron microscope was purchased from KYKY Technology Co., Ltd. JEM-1230 transmission electron microscope was obtained from JEOL, Ltd.

Preparation of lipopeptide fengycin

The fermentation liquor of *B. amyloliquefaciens* BA-16-8 was precipitated with 2 mol L⁻¹ HCl and extracted with methyl alcohol, obtaining the antibacterial coarse extraction product. This product was separated, purified, frozen, and dried via HPLC. Hence, pure products of the lipopeptide antifungal substance fengycin were obtained.

Growth curve of *P. expansum*

The growth curve of *P. expansum* was tested on the basis of the dry weight of the hyphae. *P. expansum*, which was stored on the slope, was transplanted to the potato dextrose agar (PDA) panel and cultured at 30°C for 48 h. Bacterial cakes with a diameter of 5 mm were prepared using a sterile puncher and then transplanted into the Potato dextrose broth (PDB) culture medium at 30°C at a rate of 180 r min⁻¹. The fermentation liquor was centrifuged at 10000 g for 10 min in different phases. The supernatant was eliminated, and the product was rinsed thrice with sterile water. Subsequently,

the product was dried to a constant weight at 65°C and then weighed. The growth curve of *P. expansum* was drawn with time as the x-axis and mycelium mass as the y-axis (Enebe and Babalola 2019).

Effects of fengycin on the growth of *P. expansum*

P. expansum was transplanted into the PDB culture medium. Simultaneously, different concentrations of fengycin were added, followed by 96 h of oscillation at 28°C at a rate of 180 r min⁻¹. The products were centrifuged at 10000 g for 10 min, precipitated, and weighed. The mycelium solution without lipopeptide was used as the control. Each concentration was tested thrice to determine the half maximal inhibitory concentration (IC₅₀) and minimum fungicidal concentration (MFC) of fengycin. IC₅₀ is the median inhibitory concentration; it refers to the concentration of fengycin when the dry mycelium weight of *P. expansum* is half of that of the control group. MFC refers to the minimum concentration of fengycin when *P. expansum* does not grow.

Effects of fengycin on the mycelium cell structure of *P. expansum*

Different concentrations of fengycin were added to the *P. expansum* solution in the logarithmic phase. The solution without fengycin was used as the control. The samples were cultured in a shaker for 24 h at 30°C at a rate of 180 r min⁻¹. The mycelia of different groups were collected for follow-up studies. The mycelia under different treatments were studied via TEM and SEM as previously described (Liu and Chang 2018; Pennerman *et al.* 2019).

Effects of fengycin on the nuclear dna of *p. expansum* in the electrophoretic mobility shift assay (EMSA)

The chromosomal DNA of *P. expansum* was extracted using the SK8229 kit of Sangon Biotech Co., Ltd. The extracted DNA was mixed with 20, 50, 100, 150, and 300 µg mL⁻¹ fengycin and 0.5, 1, 3, 13, and 30 µg mL⁻¹ natamycin successively. The mixture was incubated for 1 h at room temperature. Subsequently, EMSA experiment was conducted via 1% agarose gel electrophoresis. The fengycin and natamycin used in the experiment were dissolved in the binding buffer solution.

Results

Growth law of *P. expansum*

The growth curve of *P. expansum* is shown in Fig. 1. The entire growth curve conforms to the growth law of filamentous fungi. The entire growth phase includes the lag, logarithmic growth, and decline phases. Fungal strains were at the logarithmic growth period for 2–6 days, exhibiting

vigorous metabolism. Therefore, mycelia at 4 days were selected for follow-up studies.

Effects of fengycin in inhibiting the growth of *P. expansum*

The effects of fengycin concentration on the growth inhibition of *P. expansum* are presented in Table 1. Fengycin can significantly inhibit the growth of *P. expansum*. Inhibition strength increases gradually with an increase in fengycin concentration. When fengycin concentration is $50 \mu\text{g mL}^{-1}$, the inhibition rate of mycelia reaches 50%. When fengycin concentration is $150 \mu\text{g mL}^{-1}$, no mycelial growth of *P. expansum* was observed in the liquid medium. The IC_{50} of natamycin is $1.0 \mu\text{g mL}^{-1}$ and its MFC was $13 \mu\text{g mL}^{-1}$.

Effects of fengycin on the morphological structure of *P. expansum* mycelia

The morphological changes of *P. expansum* mycelial cells before and after fengycin treatment were observed via SEM. The results are shown in Fig. 2. Compared with those of the control group, the *P. expansum* mycelial cells of the experimental groups exhibit a relatively rougher surface and irregular mycelial shapes.

The effects of fengycin on the internal structures of *P. expansum* mycelial cells were observed via TEM (Fig. 3). In the control group, the mycelial cells of the pathogenic fungi have integrated cell walls, smooth and complete membrane, uniform cytoplasm, clear karyotheca and nucleolus, and distinct organelles, such as the mitochondrion. In the fengycin-treated groups, the mycelial cells do not exhibit significant thinning or thickening, but the cell membrane is deformed or partially degenerated. Cell organelles present significant changes, as manifested by the partial or complete damages to organelles, such as the cell nucleus and mitochondrion.

Effects of fengycin on *P. expansum* DNA

The effects of fengycin on *P. expansum* DNA were evaluated via EMSA through the *in vitro* combination of fengycin and natamycin with *P. expansum* DNA (Fig. 4). With the continuous increase in fengycin concentration, the migration rate of *P. expansum* DNA decreases and the band darkens gradually, while the corresponding sample hole is brightened increasingly, indicating the growth of DNA in the sample hole. Changes in migration rate are the collaborative consequences of the strong bond between fengycin and the genomic DNA of *P. expansum*. The strength of this bond is related to fengycin concentration in the mixture. At $50 \mu\text{g mL}^{-1}$ fengycin, several genomic DNA is combined partially with fengycin, resulting in changes in migration rates. Several DNA is retained at the sample holes. Band brightness is lower in the fengycin-treated

Table 1: Inhibitory effect of Fengycins against growth of *P. expansum*

Item	Half lethal dose ($\mu\text{g/mL}$)	Minimum bactericidal concentration ($\mu\text{g/mL}$)
fengycin	50.0 ± 1.2	150.0 ± 3.6
natamycin	1.0 ± 0.2	13.0 ± 0.1

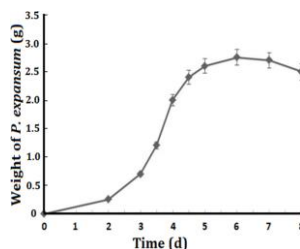


Fig. 1: The growth curve of *Penicillium expansum*

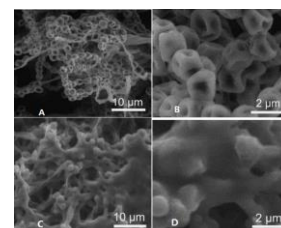


Fig. 2: SEM images of *P. expansum* with (A and B) or without (C and D) the treatment of fengycin

groups than in the control group. At $300 \mu\text{g mL}^{-1}$ fengycin, genomic DNA is completely retained in the sample holes due to the strong binding with fengycin.

In Fig. 5, the bands of *P. expansum* DNA are basically similar to those of the control group as the concentration of natamycin increases, indicating that natamycin cannot undergo *in vitro* nonspecific binding with *P. expansum* DNA, and fengycin and natamycin exert different action mechanisms on *P. expansum*. This condition may be related to the difference in structure of fengycin and natamycin. Fengycin contains polar amino acids that can facilitate its *in vitro* binding with DNA. In summary, fengycin may penetrate into the membrane and interact with the DNA in the cell nucleus of pathogens.

Discussion

To evaluate fengycin's inhibition of *P. expansum*, we investigated the effects of fengycin on the membrane of *P. expansum* mycelial cells via electron microscopy. The results demonstrated that *P. expansum* mycelial cells exhibited rough and irregular surfaces after fengycin treatment, along with different degrees of damages to internal organelles (Luo *et al.* 2019). However, the morphology of the cell wall remained basically unchanged. In addition, internal structure changes in *P. expansum* were intensified as fengycin treatment time increased, suggesting that fengycin may not only change membrane permeability, but also penetrate into cells and affect intracellular substances (Zhao *et al.* 2018). This finding requires further verification.

EMSA is frequently used to study the binding between polypeptides and DNA. The current study discussed and compared the *in vitro* binding of fengycin and natamycin with the DNA of pathogenic fungi. The results demonstrated that fengycin may undergo *in vitro* nonspecific binding with DNA, but natamycin cannot. This finding may be attributed to the difference in structures between fengycin and

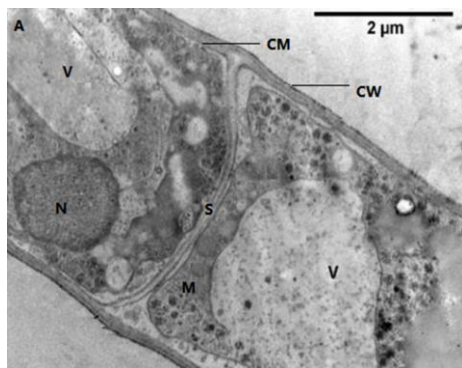


Fig. 3: The TEM images of *P. expansum* without (A) or with (B) the treatment of fengycin

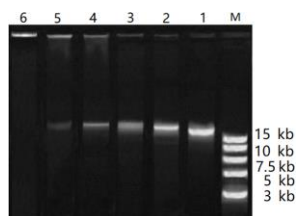


Fig. 4: The analysis of DNA-binding properties of fengycins by gel retardation assay

Note: M: marker, Lanes 1- 6 are respectively: Control group (Sterile water), 20 $\mu\text{g mL}^{-1}$ of fengycin, 50 $\mu\text{g mL}^{-1}$ of fengycin, 100 $\mu\text{g mL}^{-1}$ of fengycin, 150 $\mu\text{g mL}^{-1}$ of fengycin, 300 $\mu\text{g mL}^{-1}$ of fengycin

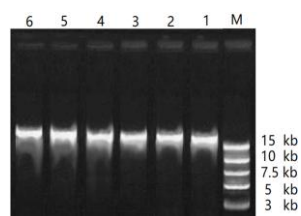


Fig. 5: The analysis of DNA-binding properties of natamycin by gel retardation assay

Note: M: marker, Lanes 1- 6 are respectively: Control group (Sterile water), 0.5 $\mu\text{g mL}^{-1}$ of natamycin, 1 $\mu\text{g mL}^{-1}$ of natamycin, 3 $\mu\text{g mL}^{-1}$ of natamycin, 13 $\mu\text{g mL}^{-1}$ of natamycin, 30 $\mu\text{g mL}^{-1}$ of natamycin

natamycin (Liu *et al.* 2019). Fengycin contains polar amino acids (e.g., Tyr, Glu, and Thr), which are absent in natamycin. These polar amino acids can combine with basic groups in DNA (Huang *et al.* 2019). Therefore, fengycin not only changes the membrane permeability of *P. expansum* mycelia but can also penetrate into cells and affect nucleic acids, inhibiting the binding of DNA and other organelles. This finding conforms with the TEM results.

Conclusion

In this study, the effects of fengycin on the morphological structure and DNA of *P. expansum* mycelia are investigated via SEM, TEM, and EMSA. A conclusion can be drawn that the anti-fungus activity of fengycin is not only limited in the membrane but may also reach other intracellular substances. This finding provides a new perspective into the antifungal mechanism of fengycin.

Acknowledgements

This work was financially supported by the state scholarship fund (China Scholarship Council Program No.10006) and Henan Provincial Science and Technology Project (182102310995 and 182102110002).

References

- Beld J, EC Sonnenschein, CR Vickery (2014). The phosphopantetheinyl transferases: Catalysis of a post-translational modification crucial for life. *Nat Prod Rep* 31:61–108
- Costa JAV, H Treichel, LO Santos, VG Martins (2018). Solid-state fermentation for the production of biosurfactants and their applications. *Curr Dev Biotechnol Bioeng* 2018:357–372
- Crossley A (1976). A versatile multi-specimen holder for processing and critical point drying of materials for examination in the scanning electron microscope (SEM). *J Microscopy* 108:349–352
- Enebe MC, OO Babalola (2019). The impact of microbes in the orchestration of plants' resistance to biotic stress: A disease management approach. *Appl Microbiol Biotechnol* 103:9–25
- Ferraz P, F Cássio, L Cândida (2019). Potential of yeasts as biocontrol agents of the phytopathogen causing cacao witches' broom disease: Is microbial warfare a solution? *Front Microbiol* 10:1–13
- Fu RM, WH Xing, H Zhang, LQ Zhang, WL Chen (2016a). Breeding of antagonistic bacteria against *Penicillium expansum* and study on its inhibition mechanism. *Sci Technol Food Indust* 5:154–158
- Fu RM, F Yu, HP Chang, H Zhang, WL Chen (2016b). Isolation, and characterization of an antagonistic bacterium against *Penicillium expansum*. *Microbiol Chin* 43:1–10
- Huang J, Y Pang, F Zhang, Q Huang, M Zhang, S Tang, H Fu, P Li (2019). Suppression of *Fusarium wilt* of banana by combining acid soil ameliorant with biofertilizer made from *Bacillus velezensis* H-6. *Eur J Plant Pathol* 154:585–596
- Liu CY, Z Chang (2018). Identification of the biocontrol strain LB-2 and determination of its antifungal effects on plant pathogenic fungi. *J Plant Pathol* 100:25–32
- Liu YN, J Lu, J Sun, FX Lu, XM Bie, ZX Lu (2019). Membrane disruption and DNA binding of *Fusarium graminearum* cell induced by C16-Fengycin A produced by *Bacillus amyloliquefaciens*. *Food Cont* 102:206–213
- Luo AW, JQ Bai, R Li, YM Fang, L Li, D Wang, L Zhang, J Liang, TZ Huang, LP Kou (2019). Effects of ozone treatment on the quality of kiwifruit during postharvest storage affected by *Botrytis cinerea* and *Penicillium expansum*. *J Phytopathol* 167:470–478
- Mohammadi B, M Salouti (2015). Extracellular bioynthesis of silver nanoparticles by *Penicillium chrysogenum* and *Penicillium expansum*. *Synth React Inorg Metal-Org Nano-Metal Chem* 45:844–847
- Moosa A, A Farzand, ST Sahi, ML Gleason, SA Khan, X Zhang (2019). First report of postharvest fruit rot of *Citrus reticulata* 'Kinnow' caused by *Penicillium expansum* in Pakistan. *Plant Dis* 103:155
- Pennerman KK, JB Scarsella, GH Yin, SST Hua, TG Hartman, JW Bennett (2019). Volatile 1-octen-3-ol increases patulin production by *Penicillium expansum* on a patulin-suppressing medium. *Mycotox Res* 2019: 1–12
- Rozas EE, MA Mendes, MR Custódio, DC Espinosa, CAO Nascimento (2019). Self-assembly of supramolecular structure based on copper-lipopeptides isolated from e-waste bioleaching liquor. *J Hazard Mater* 368:63–71
- Srikhong P, K Lertmongkonthum, R Sowanpreecha, P Remngsamran (2018). *Bacillus* sp. strain M10 as a potential biocontrol agent protecting chili pepper and tomato fruits from anthracnose disease caused by *Colletotrichum capsici*. *Biocontrol* 63:833–842
- Tanaka K, I Atsushi, N Hiromitsu (2014). Isolation of anteiso-C17, iso-C17, iso-C16, and iso-C15 Bacillomycin D from *Bacillus amyloliquefaciens* SD-32 and their antifungal activities against plant pathogens. *J Agric Food Chem* 62:1469–1476
- Villegas-Escobar V, LM González-Jaramillo, M Ramirez, RN Moncada, L Sierra-Zapata, S Orduz, M Romero-Tabarez (2018). Lipopeptides from *Bacillus* spp. EA-CB0959: Active metabolites responsible for *in vitro* and *in vivo* control of *Ralstonia solanacearum*. *Biol Cont* 125:20–28
- Zhao JF, C Zhang, ZX Lu (2018). Differential proteomics research of *Bacillus amyloliquefaciens* and its genome-shuffled saltant for improving fengycin production. *Braz J Microbiol* 49:166–177